CrossMark

Potentials for expanding dry-land agriculture under global warming in water-stressed regions: a quantitative assessment based on drought indices

Fahimeh Shahsavari[1] · Fatemeh Karandish[1] · Parviz Haghighatjou[1]

Abstract

Agricultural sustainability under the warming climate highly depends on limiting the extreme use of the blue water resources within the irrigated lands, and instead, optimally applying green water resources within the expanded rainfed lands. In this research, potentials for expanding dry farming under climate change were analyzed in five climatic zones of Iran, based on the future projections of basic weather data and drought indices under 20 general circulation models (GCMs) and four emission scenarios, including RCP2.6, RCP4.5, RCP6.5, and RCP8.5. Drought indices included aridity index (AI), expressed as precipitation divided by evapotranspiration, and green water deficit (GWD), expressed as precipitation minus mines evapotranspiration. While annual predictions show a general increase in both precipitation and air temperature over the 2041–2070 period, given results at the monthly scale well revealed the spatial and temporal non-uniformity in the climate change projections. Such heterogeneities, together with those presented for different GCMs and RCPs, well indicated the importance of undertaking a wide range of uncertainties when implementing long-term planning. Based on GWD and AI, the arid and semi-arid regions, the backbone of the rainfed agriculture in Iran, are the most vulnerable to global warming. In these regions, green water availability will reduce by 0.8–167.5% especially within the wet seasons, and drought severity will increase by 0.1–33.2% through the rainfed cropping cycles. On the other hand, future climate may provide new opportunities for expanding dry farming within the hyper-arid region, which is now the most water-stressed region of the country. In this region, global warming projections show a positive increase of 0.3–146.2% in green water availability, and a reduction of 5.1–266.4% in drought severity. However, the humid region remained as the most suitable region for producing rainfed crops, although being widely allocated to irrigated-rice production under current condition. Based on the results, achieving sustainable dryland agriculture highly depends on regionally prioritizing susceptible area for dry farming, since the criteria indices showed an extreme spatial and temporal variability over the mid twenty-first century.

1 Introduction

While being unavoidable under rapid population growth, growing irrigated agriculture is a serious threat to water and food security, especially within the highly water-stressed regions, which consequently results in serious socioeconomic hazards may be expected as well (Tigkas et al. 2018; Li et al. 2017; Zhang et al. 2017a; Wegren 2011; Zhao and Running 2010). Under such circumstances, developing dry farming may be considered as a rational solution for alleviating the

severity of pressure on the limited blue water resources. Implementing such targets may be of higher importance in the coming future, since previous researchers reported a decreasing trend in the global blue water availability over the dry seasons under global warming (Tabari et al. 2015). While improving future irrigated-agriculture has been widely investigated (e.g., Darzi-Naftchali and Karandish 2017; Karandish et al. 2017a, b), less attention has been paid to investigate potentials for expanding dry farming under global warming aiming at increasing the contribution of green water resources within the agricultural lands.

Various factors affect regional capability for expanding dry farming, among which the site-specific green water availability may be of priority, since crop water requirement over the rainfed cropping cycle is fully supplied by green water resource. Hence, numerous indices have been developed over

✉ Fatemeh Karandish
  Karandish_h@yahoo.com; F.karandish@uoz.ac.ir

[1] Water Engineering Department, University of Zabol, Zabol, Iran

the past decades for determining site-specific climatic-suitability of a region for rainfed cropping (WMO and GWP 2016), among which two indices are of higher importance: green water deficit (GWD) and aridity index (AI). GWD, described as the difference between precipitation and potential evapotranspiration (Karandish and Mousavi 2018), is a proper index by which the period of water deficit and water surplus could be determined (Shifteh Some'e et al. 2013; Tabari and Aghajanloo 2013; Tabari and Hosseinzadeh Talaee 2013). In the other word, sustainable water availability may be determined when GWD is calculated (Milly et al. 2005). AI, defined as precipitation divided by evapotranspiration (UNESCO 1979), is referred as a proper indicator of drought especially when agricultural drought is of priority (Keyantash and Dracup 2002; Paltineanu et al. 2007; Tabari and Aghajanloo 2013; Wang et al. 2014).

Both AI and GWD may vary by space and time. Over the past decades, a significant temporal variation in GWD and AI indices has been reported in different regions of the world (Salark and Mahmood-Agha 2017; Zhao et al., 2017; Zhang et al. 2017b; Moral et al. 2016; Muhire and Ahmed 2016; Ashraf et al. 2014; Ahani et al. 2013; Shifteh Some'e et al. 2013; Liu et al. 2013). Being highly depended on the climate variability (Liu et al. 2017; Gebremedhin et al. 2017; Zhang et al. 2017b; Dong et al. 2013), temporal variations of AI and GWD may be of higher importance over the future periods, since a pronounced change in the climate variables has been reported by the IPCC (IPCC 2013). In 2007, IPCC reported that globally, earths' surface temperature experienced a 1 °C increase over the last twentieth century, and will experience a 1.1–6.4 °C more increase over the twenty-first century. Hence, it is an essential to first anticipate the projected AI, and GWD under global warming when implementing the long-term plans for expanding rainfed areas is considered.

Despite of a serious focus on estimating global warming projections into basic weather data such as precipitation and cardinal temperatures (e.g., Karandish et al. 2017a; Karandish and Mousavi 2018; Trnka et al. 2004), less attention has been paid to predict the projected AI and GWD in the future periods. A few researchers investigated the long-term effects of climate change on AI and GWD in different parts of the world over the twenty-first century, mainly based on the given results for a few GCMs and emission scenarios (Liu et al. 2017; Gebremedhin et al. 2017; Zhang et al. 2017b; Karandish and Mousavi 2018; Dong et al. 2013). They generally believe that there is a large spatial and temporal heterogeneities in climate change projections. Hence, the main focus of this research is to find out the dry farming suitability in different climatic regions of a highly water-stressed country under climate change. In this regard, historical variation and climate change projections of the basic weather data, as well as AI and GWD, are analyzed within five climatic regions of Iran, and then, the rainfed cropping suitability are quantitatively assessed over the mid twenty-first century.

2 Methods and data

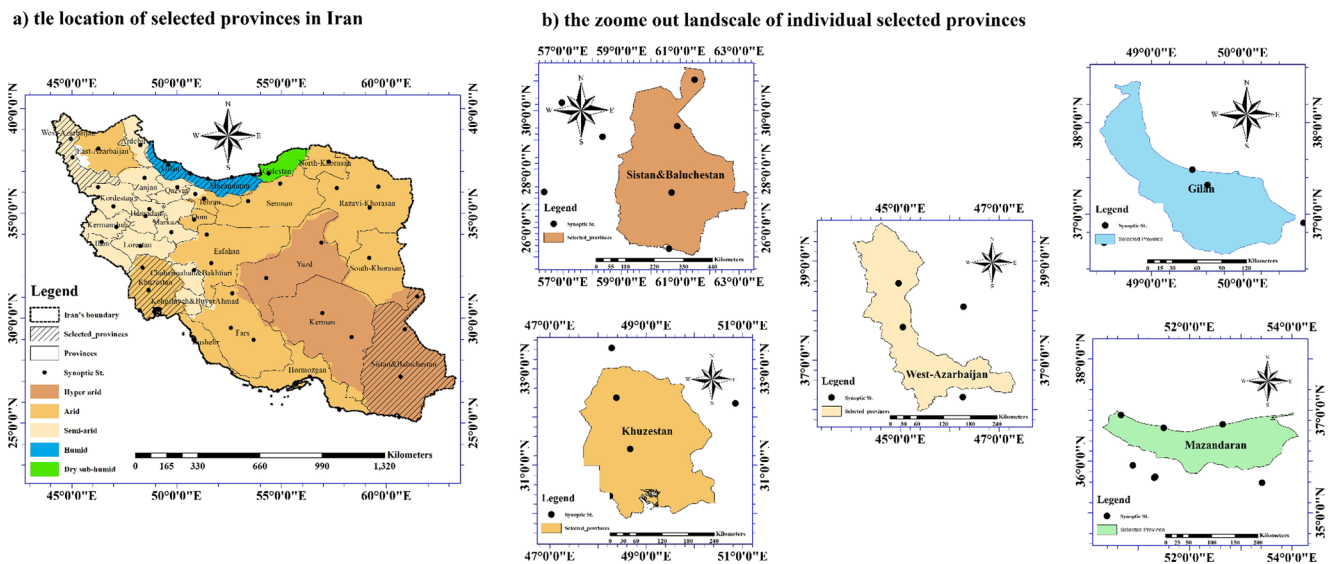### 2.1 Study area and data collection

Iran, the second large country in the Middle East, is classified as a highly water-stressed country in the world. Results of De-Martine classification method reveal that Iran consists of five climatic zones: hyper arid, arid, semi-arid, humid, and dry sub-humid regions (Karandish and Mousavi 2018; Karandish et al. 2017a). With a focus on the contribution of different provinces to national production and their climatic properties, we selected five provinces of Sistan and Baluchestan (located within the hyper arid region), Khuzestan (located within the arid region), West-Azarbaijan (located within the semi-arid region), Mazandaran (located within the humid region), and Golestan (located within the dry sub-humid region) (Fig. 1). These provinces face serious water quality and quantity challenges (Karandish and Hoekstra 2017) and are mostly the backbone of Iran's agriculture.

Over the base period of 1975–2005, daily weather data were collected in 13 synoptic stations located within five selected provinces (IRIMO 2017). Besides, the agricultural data, differentiated by the irrigated or rainfed farming, and including cropping pattern, cropping calendar, harvested area, crop yield, and all other data related to field management practices were collected from Iran's Ministry of Agricultural Jihad (IMAJ 2017).

2.2 Projections of climate change

Based on the 5th report of IPCC, the projections of climate variables in the future periods were obtained. These projections were then downscaled under four Representative Concentration Pathways (RCPs), RCP2.6 (low), RCP4.5 (intermediate), RCP6.5 (high), and RCP8.5 (very high greenhouse gas concentrations scenario), over the period 2041–2070. The projections of global warming into essential weather data (including air temperature, precipitation, solar net radiation, wind speed, atmosphere pressure, and relative humidity) were then generated for 20 general circulation models (GCMs), described in Table 1.

The change factors method, introduced by Jones et al. (1997), which is widely used by the other researchers (Darzi-Naftchali and Karandish 2017; Trzaska and Schnarr 2014), was applied to statistically downscale the selected climate variables in 13 selected synoptic stations. The relation between current climate data and future GCMs projections, called change factor, was calculated by Eqs. 1 and 2 for all climatic parameter (Jones et al. 1997), except for air temperature, for

a) tle location of selected provinces in Iran

b) the zoome out landscale of individual selected provinces

Fig. 1 The location of the selected provinces within Iran (**a**), and the zoom out of the selected provinces and synoptic stations by individual (**b**)

Table 1 Global climate models (Source: Chiyuan, et al. (2014))

Model	Source
ACCESS 1.0	Common Wealth Scientific and Industrial Research Organization and Bureau of Meteorology, Australia
BCC-CSM1.1	Beijing Climate Center, China Meteorological Administration, China
BNU-ESM	Beijing Normal University, China
CanESM	Canadian Center for Climate Modeling and Analysis, Canada
CCSM4	National Center for Atmospheric Research (NCAR), USA
CESM1.0-BGC	National Center for Atmospheric Research (NCAR), USA
CISRO-MK3	Australian Common Wealth Scientific and Industrial Research Organization
GFDL-ESM2G	Geophysical Fluid Dynamic Laboratory, USA
GFDL-ESM2M	Geophysical Fluid Dynamic Laboratory, USA
HadGEM2-CC	Met office Hadley Center, UK
HadGEM2-ES	Met office Hadley Center, UK
inmcm4	Institute of Numerical Mathematics, Russian Academy of Sciences
IPSL-CL5A-LR	Institute Pierre-Simon Laplace, France
IPSL-CL5A-MR	Institute Pierre-Simon Laplace, France
MIROC	Japan Agency for Marin-Earth Science and Technology, Atmosphere and Ocean Research Institute (University of Tokyo Japan)
MIROC-ESM	Japan Agency for Marin-Earth Science and Technology, Atmosphere and Ocean Research Institute (University of Tokyo Japan)
MPI-ESM-LR	Max Plank Institute for Meteorology (MPI-M), Germany
MPI-ESM-MR	Max Plank Institute for Meteorology (MPI-M), Germany
MRI-CGCM3	Meteorological Research Institute of Japan
Nor-ESM1-M	Norwegian Climate Center, Norway

which the Eqs. 3 and 4 was applied (Trzaska and Schnarr 2014), as in the following:

$$\Delta P_i = \left(\frac{\overline{P}_{\text{GCM,fut},i}}{\overline{P}_{\text{GCM,base},i}} \right) \tag{1}$$

$$\Delta T_i = \left(\overline{T}_{\text{GCM,fut},i} - \overline{T}_{\text{GCM,base},i} \right) \tag{2}$$

where, ΔP_i is the dimensionless monthly change factor for the considered climatic data (p), $\overline{P}_{\text{GCM,fut},i}$ and $\overline{P}_{\text{GCM,base},i}$ are, respectively, the monthly average future simulated and the historical values of the considered climatic data over the period, ΔT_i is the dimensionless monthly change factor for air temperature, and $\overline{T}_{\text{GCM,fut},i}$ and $\overline{T}_{\text{GCM,base},i}$ are, respectively, the monthly average future simulated and the historical values of the air temperature over the period. These change factors were calculated at the monthly time scale ($i = 1$–12).

2.3 Aridity index and green water deficit

Over the base and the future periods, FAO-Penmann Monteith Equation was applied to calculate daily potential evapotranspiration as in the following (Allen et al. 1998):

$$\text{ET}_O = \frac{0.408(R_n - G) + \gamma \left(\frac{900}{T + 273} \right) \times U_2 \times (e_s - e_a)}{\Delta + \gamma(1 + 0.34U_2)} \tag{3}$$

where, Δ is the slope of the vapor pressure curve (kPa $^\circ$C^{-1}), R_n is the net radiation at the crop surface (MJ m^{-2} day^{-1}), γ is the psychrometric constant (kPa $^\circ$C^{-1}), T is the average air temperature ($^\circ$C), U_2 is the average wind speed (m s^{-1}) at 2 m height, G is the soil heat flux density (MJ m^{-2} day^{-1}), e_s

is the saturation vapor pressure (kPa), and e_a is the actual vapor pressure (kPa).

Thereafter, monthly aridity index (AI) and monthly green water deficit (GWD) were calculated based on the Eqs. 3 and 4 (Karandish and Mousavi 2018; UNESCO 1979).

$$\begin{cases} \text{AI} = \dfrac{P_{\text{month}}}{\text{ET}_{\text{Omonth}}} \\ \text{GWD} = P_{\text{month}} - \text{ET}_{\text{Omonth}} \end{cases} \quad (4)$$

where, P_{month} is monthly precipitation (mm month^{-1}), and $\text{ET}_{\text{Omonth}}$ is monthly ETo (mm month$^{-1)}$.

3 Results and discussion

3.1 Projections to basic climatic variables

Air temperature Figure 2 represents monthly variations of minimum (Tmin) and maximum (Tmax) air temperature over the base period, and over the mid twenty-first century (2041–2070) based on the average results of the 20 GCMs for all RCPs. While given results for the average of all ensembles presented a large spatial and temporal variability in future projections, an obvious difference in future projections was revealed for different models and RCPs. This is mainly resulted from the different assumptions related to economic, social, and environmental models in these scenarios (Karandish et al. 2017a). Such result is an indication of uncertainty in T projections in the future period, which may be considered as a great threat to the long-term planning if such panning is made based on given results for a few RCPs or GCMs.

Regardless of the climatic regions, Tmin is projected to a − 92% up to 60% change under global warming, with generally the lowest (from − 79 to 41%) and the largest (from − 92 to 52%) change under RCP2.6 and RCP8.5, respectively. The elevated CO_2 seems to expose the largest change in Tmin over the wet seasons. Under RCP2.6 and RCP4.5, the hyper arid region may experience the largest change in Tmin, with an overall average of − 31% and − 23%, respectively, while the humid region experiences the lowest change in Tmin, with an overall average change of − 2% and 9%, respectively. Under RCP6.5 and RCP8.5, climate change projected the lowest and the largest change in Tmin within the arid and dry sub-humid regions, respectively.

Based on the average results of the 20 GCMs for each scenario, and compared to the base period, climate change projections show a positive increase of the monthly Tmax within the arid regions, accounted for 3–40%, the largest of which occurred over the wet seasons for all RCPs. While no constant pattern is followed, climate change projections show both positive and negative change of the monthly Tmax within the other climatic regions. The humid and dry sub-humid

Fig. 2 Temporal variation of monthly minimum (Tmin) and maximum ▶ (Tmax) air temperature over the based period (1975–2005), and over the future period (2041–2070) based on the ensemble average of the 20 GCMs for each scenario

regions, which are the most suitable climatic regions for expanding dry farming under current condition, tend to get warmer over the 2041–2070 period, which is justified by the fact that the wet seasons in these regions will experience a positive increase in their monthly Tmax, while the dry seasons will usually experience a considerable reduction in monthly Tmax. Exception was for RCP8.5, under which a colder climate is expected.

Precipitation and ETo The average results of the 20 GCMs for each scenario shows a positive increase in annual P in different climatic regions, accounted by 0.3% (within the dry sub-humid region under RCP4.5) to 75% (within the hyper-arid region under RCP8.5) (Table 2). At the national scale and based on the monthly calculated values, Iran received 60–328 mm month^{-1} precipitation over the base period (Fig. 3). During the 2041–2070 period, monthly national P generally increase by 3.2% (during December under RCP2.6) to 103.9% (during April under RCP8.5), despite of a slight precipitation reduction of 3.4–19.6% over a few months.

While the pattern of monthly P variations in Fig. 3 is an indication of a non-uniform temporal projected effect of climate change scenario on P, the non-uniform spatial change in monthly P under global warming is also diagnosed when considering monthly P projections in different climatic regions. With an accounted range of 0.3–354%, regional downscaled P over the 2041–2070 period well represents a general increase in monthly P within the hyper-arid, arid, and humid regions. Compared to the base period, monthly P may increase by 2.7–71.8% within the dry sub-humid region over the March–July period, while it may decrease by 0.8–35.5% over the other months. In the semi-arid region, which is responsible for a large contribution of annul agricultural production in Iran, climate change mainly results in annual P reduction compared to the 1975–2005 period, accounted for 1.5–34.5%. The exceptions were for the period February–October under RCP8.5, May–June under RCP2.6, April–June and October under RCP4.5, and May–Jul and October–November under RCP6.5.

Over the base period, the overall average annual ETo in the selected regions was 146 mm, while during 2041–2070, overall average annual ETo reaches to 148 mm under RCP2.6, 151 mm under RCP4.5, 144 mm under RCP6.5, and 139 mm under RCP8.5. At the annual scale, each part of the country showed their own style of projections. General increasing trend in annual ETo under global warming was observed in the hyper arid (34–75%) and dry sub-humid region (45–62%), with the lower limits under RCP2.6 and the upper
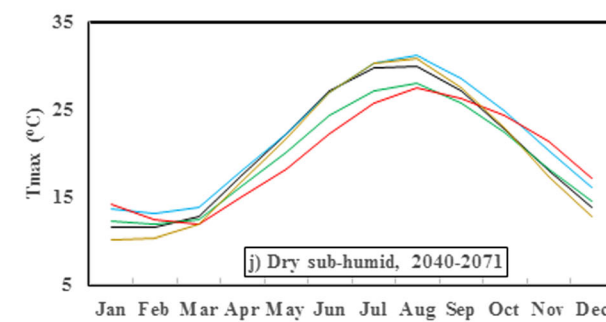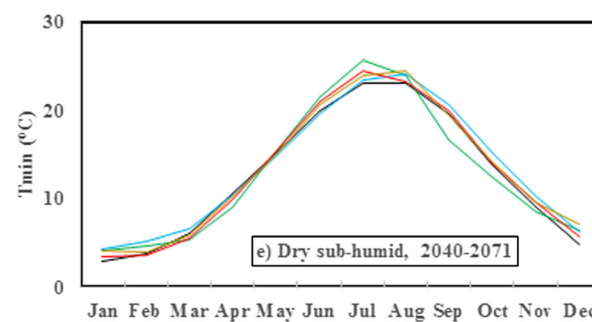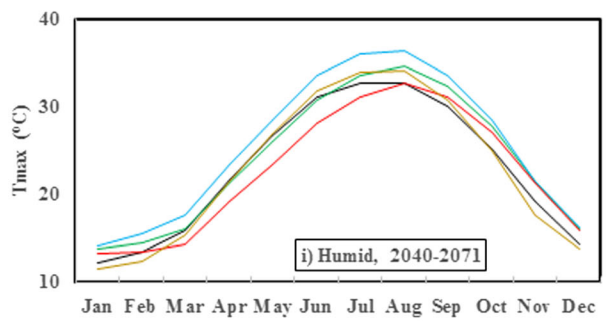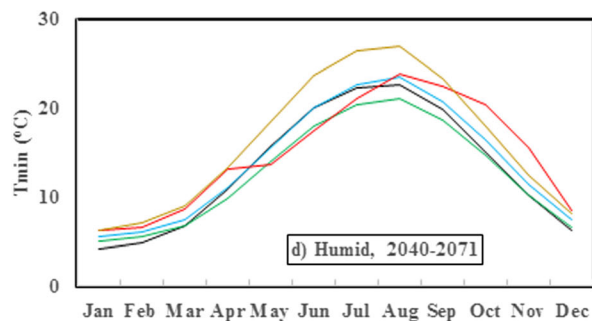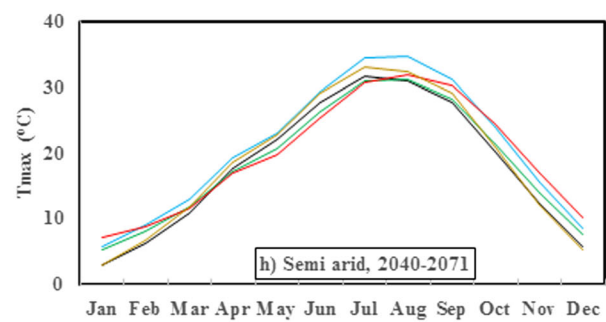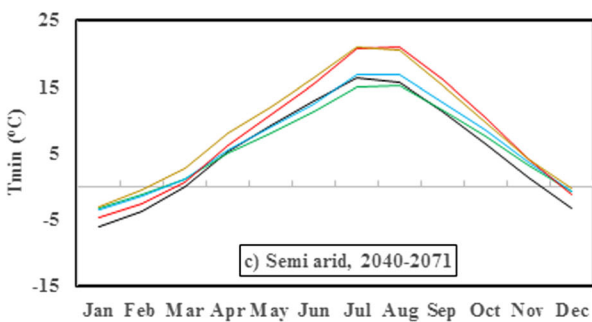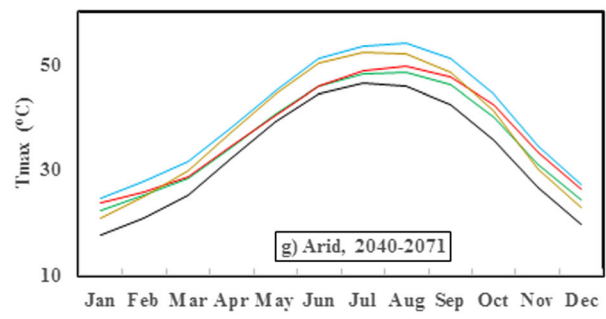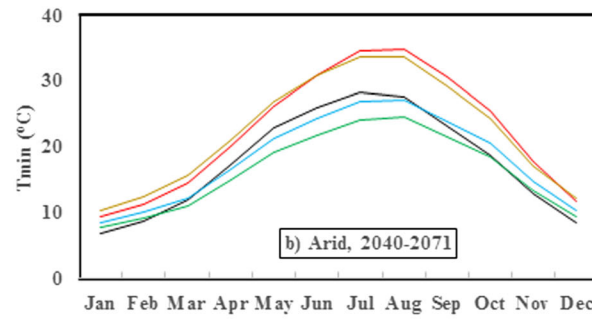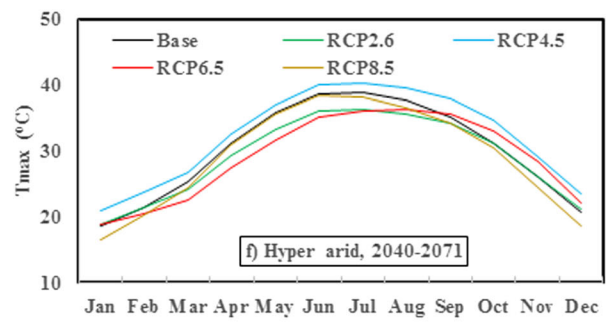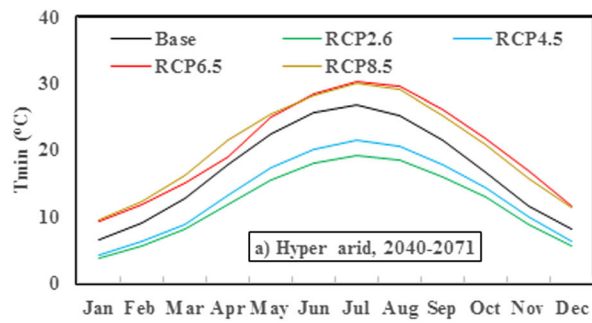
Table 2 Annual climatic parameters and drought indices within different climatic regions and in Iran as a whole, over the base (1975–2005) and future period (2041–2070). i.e., the reported values for the future period is calculated based on the average of the 20 GCMs for each scenario

Climate region	Period	Tmin	Tmax	Pr	ETo	GWD	AI
Hyper arid	Base	17.1	30.1	98	1120	− 1022	0.1
	RCP2.6	12.1	29.0	133	1048	− 915	0.1
	RCP4.5	13.4	32.2	148	1165	− 1017	0.1
	RCP6.5	20.4	29.0	166	1086	− 920	0.2
	RCP8.5	20.5	29.1	171	1064	− 893	0.2
Arid	Base	17.7	33.1	274	999	− 725	0.3
	RCP2.6	16.3	36.3	282	986	− 704	0.3
	RCP4.5	18.1	40.3	314	1095	− 782	0.3
	RCP6.5	22.3	37.3	273	1054	− 781	0.3
	RCP8.5	22.3	37.9	305	1038	− 733	0.3
Semi-arid	Base	5.9	18.0	331	842	− 511	0.4
	RCP2.6	6.5	18.6	309	780	− 471	0.4
	RCP4.5	7.2	20.6	344	867	− 523	0.4
	RCP6.5	8.7	19.5	324	853	− 529	0.4
	RCP8.5	9.3	18.7	407	852	− 446	0.5
Humid	Base	13.3	20.3	1159	769	390	1.5
	RCP2.6	12.6	19.4	1531	705	826	2.2
	RCP4.5	14.0	21.6	1701	783	918	2.2
	RCP6.5	14.8	19.7	1719	758	961	2.3
	RCP8.5	16.1	20.0	1875	745	1131	2.5
Dry sub humid	Base	12.7	22.9	562	716	− 154	0.8
	RCP2.6	12.8	24.0	590	683	−93	0.9
	RCP4.5	13.4	25.4	564	697	− 133	0.8
	RCP6.5	13.0	22.6	538	667	− 130	0.8
	RCP8.5	13.2	22.9	549	670	− 121	0.8
Iran	Base	13.3	24.9	2423	4446	− 2023	0.5
	RCP2.6	12.0	25.5	2846	4202	− 1356	0.7
	RCP4.5	13.2	28.0	3070	4607	− 1537	0.7
	RCP6.5	15.9	25.6	3020	4418	− 1398	0.7
	RCP8.5	16.3	25.7	3307	4369	− 1062	0.8

limits under RCP8.5. Despite of a general increase in regional ETo within the other regions, climate change may project a slight reduction in annual ETo in the arid and semi-arid regions under RCP2.6, and in the humid region under RCP6.5 and RCP8.5 scenarios.

More non-uniformity in the climate change projections is revealed when considering temporal variation of monthly ETo within different climatic regions over the base and the future period. At the monthly scale, ETo reduction is more likely to happen within the dry sub-humid region, accounted for 1.4–11.8%, with the highest reductions over April–June and November–December periods. As a general logic, Fig. 3 demonstrates that climate change projection into monthly ETo within a specific region is mainly controlled by the selected

Fig. 3 Temporal variation of monthly precipitation (P) and potential ▶ evapotranspiration (ETo) over the based period (1975–2005), and over the future period (2041–2070) based on the ensemble average of the 20 GCMs for each scenario
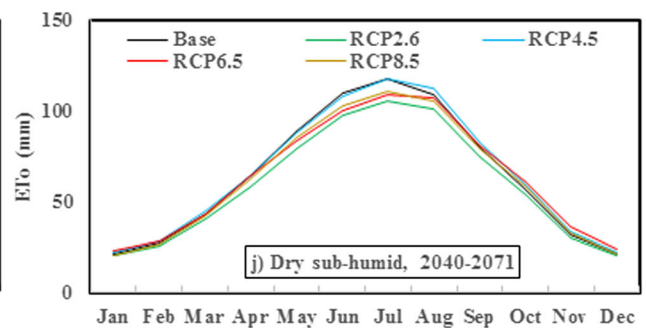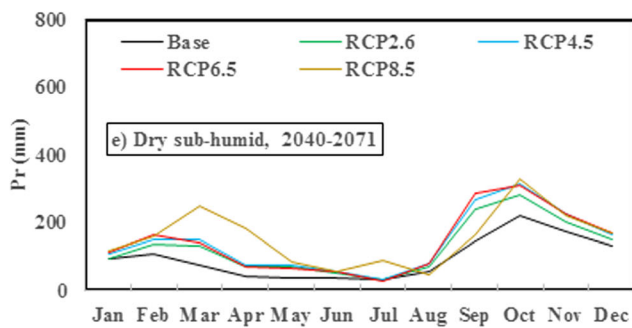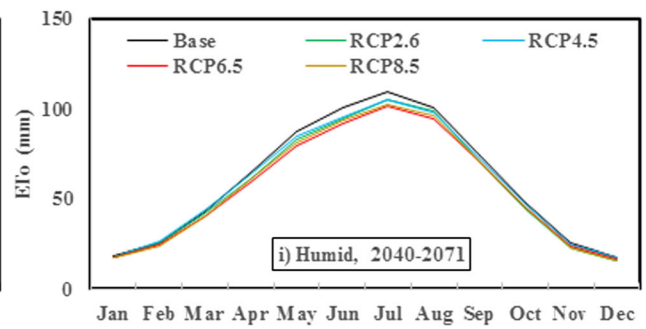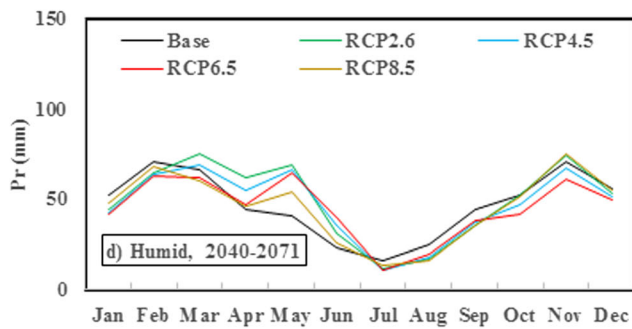
RCP scenario, rather than by the considered months. Compared to the base period, RCP4.5 within the hyper arid region, RCP4.5 and RCP6.5 and RCP8.5 within the arid and semi-arid region, and RCP4.5 and RCP6.5 within the humid region, are likely to project a general increase in monthly ETo, and ETo reduction is likely to happen in the other case.
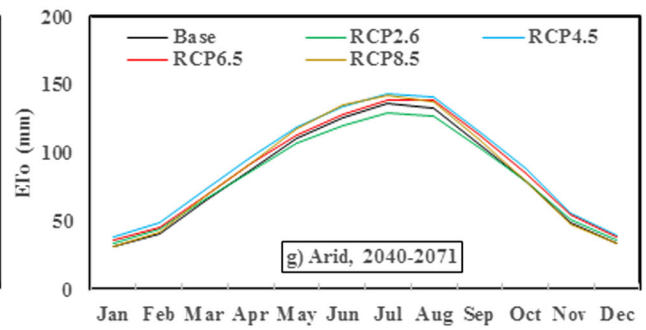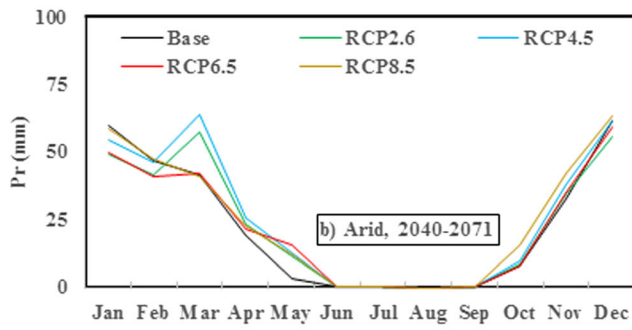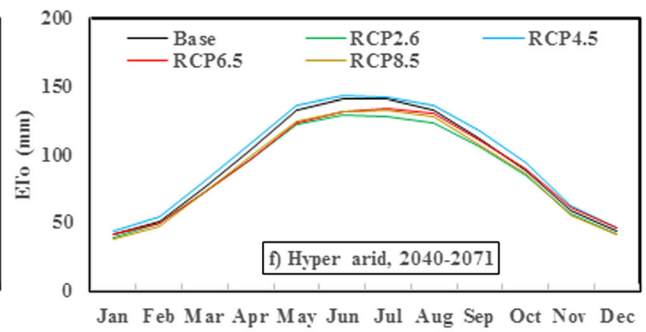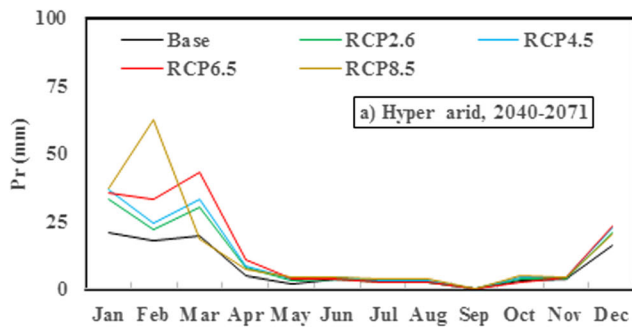
3.2 Projections to GWD and AI

Green water deficit Based on the average results of the 20 GCMs for each scenario, annual and monthly green water deficit (GWD) were calculated at the national and the regional scales (Table 2, Fig. 4). With the definition of "P-ETo," negative GWD is a sign of green water scarcity within a regions, in which ETo may exceed P (ETo > P). Table 2 shows that at the national scale, the negative consequences of climate change on ETo may be compensated by increased P, since GWD is supposed to be reduced by 24.0% (under RCP4.5) to 47.5% (under RCP8.5). Increased annual green water availability is more evident within the humid region, which is now the most water abundant region of the country. In this region, global warming projects a 112–190% increase into annual GWD over mid twenty-first century. Arid and semi-arid region seems to be the most vulnerable regions to the elevated CO_2 in the future period, where annual GWD is likely to decrease by 1.1–7.8%.

Monthly GWD assessment, however, is a more proper index for analyzing dry farming suitability within a region, since it reveals real times with surplus green water (P > ETo). In a general point of view, the hyper arid and humid regions are expected to experience wetter years over the period 2041–2070, since green water availability will increase by 0.3–713%, with the upper limits over the January–March period in the hyper arid regions, and over the February–April period in the humid region. However, the other regions, where agriculture is of a significant priority, may experience drier condition in the future, among which, the semi-arid region may experience a higher pressure on its limited blue water resources due to a 0.8–115.7% increase in green water deficit over the 2041–2070 period. Water scarcity in these regions is more evident over the wet seasons.

Aridity index (AI) AI, calculated by dividing P by ETo, is introduced as a drought index by which the situation of food security may be anticipated since crop production is highly depended on green/blue water availability over the cropping cycles (Muhire and Ahmed 2016). An AI < 1 may be a robust estimation of water scarcity since it denotes that P < ETo over

a) Hyper arid, 2040-2071
f) Hyper arid, 2040-2071
b) Arid, 2040-2071
g) Arid, 2040-2071
c) Semi arid, 2040-2071
h) Semi arid, 2040-2071
d) Humid, 2040-2071
i) Humid, 2040-2071
e) Dry sub-humid, 2040-2071
j) Dry sub-humid, 2040-2071
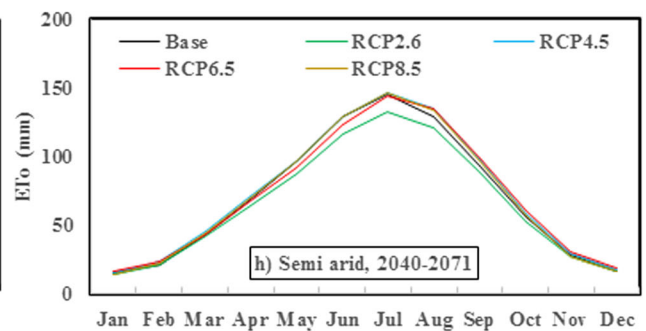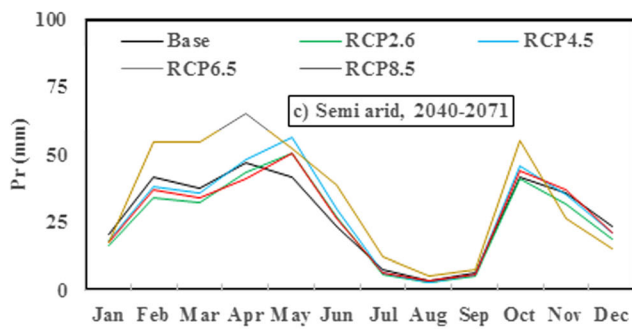
the study period. During the base period, annual AI within the country varied in the range of 0.1 (within the hyper arid region) to 1.5 (within the humid region). Regardless of a few exceptions, annual AI at the regional scale is expected to increase by 0.9–84.2% under global warming, indicating higher water availability in the future. Such increase is more evident within the hyper arid and humid regions, in which annual AI may increase by 44.1–84.2%. Varying in the range of 0.3–0.9 over the 2041–2070 period, projected annual AI may increase by 0.9–21.4% within the other climatic regions.

Monthly analysis of the AI projections, however, well demonstrate both temporal and spatial non-uniform projected effects of climate change. Global warming projections show a positive increase in monthly AI within the humid region, accounted for 5.2–329.4%, and within the hyper arid region, accounted for 5.1–266.4%. In these regions, May and September may experience the highest increase in AI over the 2041–2070 period. In the arid region, global warming projections show a general increase of 0.8–340.7% in monthly AI over the period March–November, while it is likely to have a 0.1–26.4% lowered monthly AI in January, February, and December. Nevertheless, agriculture is highly threatened within the semi-arid region, in which monthly AI is expected to have a 2.5–33.2% reduction under climate change, except for a few cases. The exception were mainly for April–Jun, where a positive projections of 0.6–66.6% in monthly AI is anticipated. Except for the March–June period, the recued monthly AI under global warming is also expected within the dry-sub-humid region.

3.3 Future perspectives dry farming

Based on the national statistics in 2010, 60% and 32% of total rainfed lands are located within the arid and semi-arid regions of the country, respectively, from which 55% and 22% of national rainfed production are produced, respectively. The humid region ranked next, where 6% of the total rainfed agricultural lands of the country are located in, which supply 12.5% of rainfed production in Iran. With the contributions of 2.3% and 0.2% in total rainfed harvested area, and 10.5% and 0.7% in total rainfed production, the dry sub-humid and hyper arid regions are, respectively, considered as the most unsuitable regions for dry farming. Such analysis well indicates that future climate of the arid and semi-arid regions may determine the potentials for expanding dry farming in Iran in the future. On the other hand, improved climatic condition in the other regions under global warming may also be a sign of potentials for expanding rainfed lands within these regions.

To analyze regional rainfed suitability over the 2041–2070 period, we calculated the number of months with increased (or decreased) GWD and AI, based on the average projections of the 20 GCMs and four RCPs scenario, and results are presented in Fig. 5. Based on the projected AIs, the arid and semi-arid
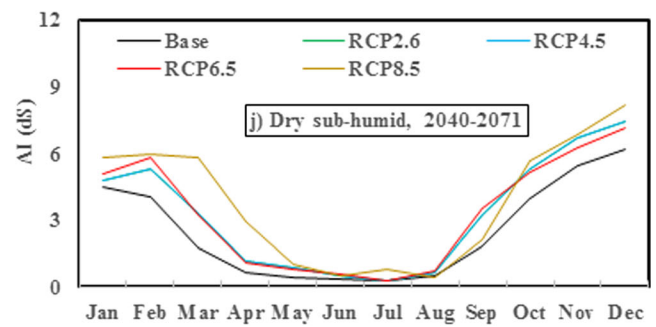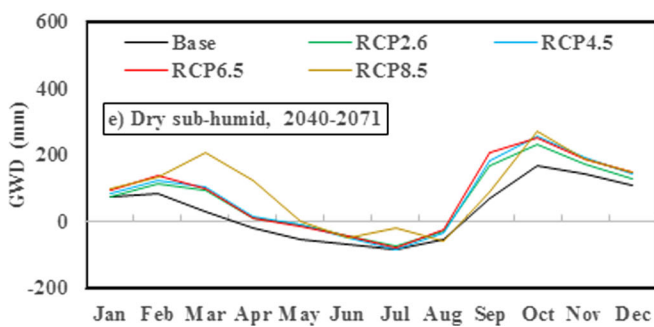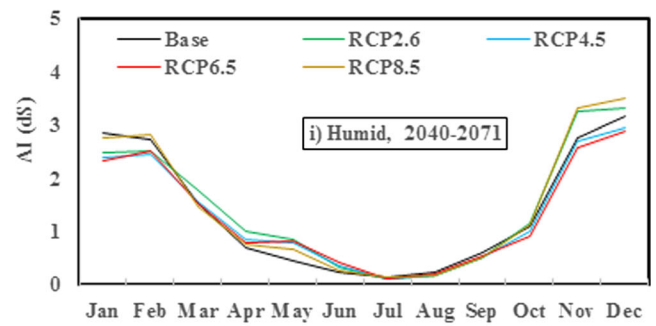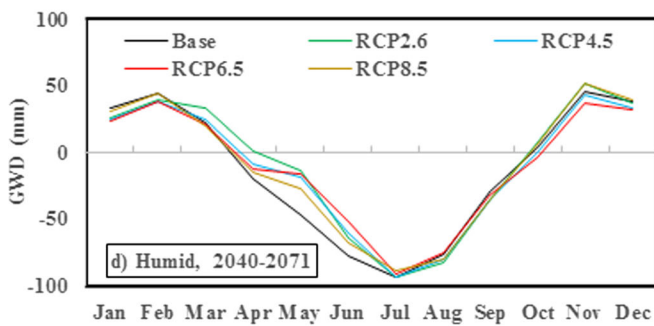
Fig. 4 Temporal variation of monthly green water deficit (GWD) and ▶ aridity index (AI) over the based period (1975–2005), and over the future period (2041–2070) based on the ensemble average of the 20 GCMs for each scenario

regions are expected to experience wetter condition over the period March–October under climate change, while the severity of aridity in these regions is supposed to be increased during late autumn and early winter. Regarding GWD, increased water availability within the arid and semi-arid regions is only expected within a few months over the late winter and early spring. Based on the national statistics, the cropping cycle of most of the rainfed crops in Iran is over the October–May period (Karandish and Hoekstra 2017), while the most crop water requirement is mainly supplied by precipitation occurred over the autumn and winter periods. Such statistics, together with given results for AI and GWD variations in Fig. 5, well demonstrate the vulnerability of dry farming under climate change within the arid and semi-arid regions. On the other hand, more potentials for expanding dry fa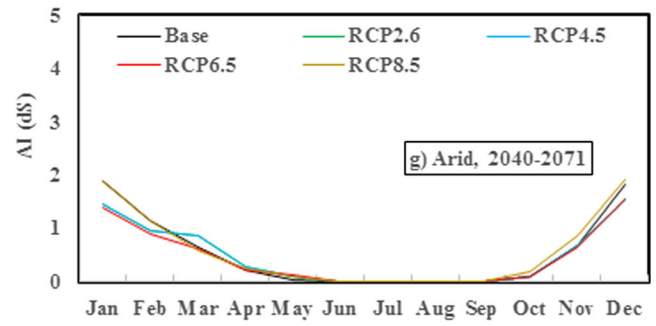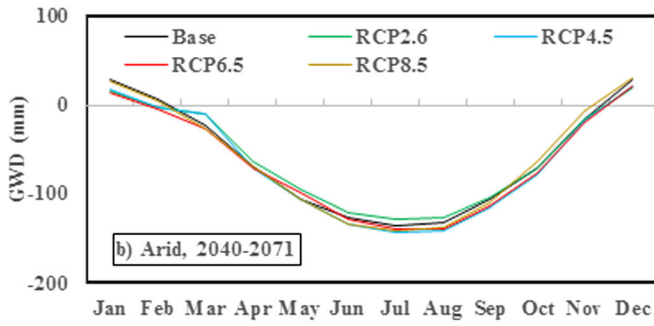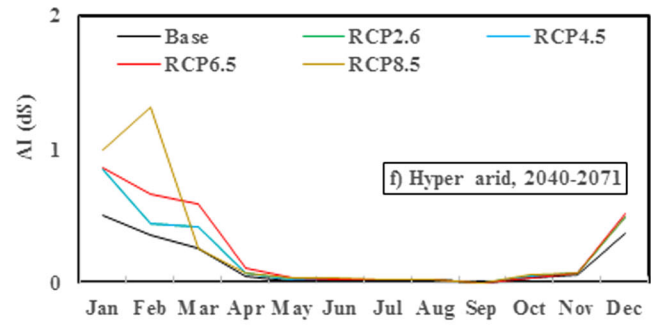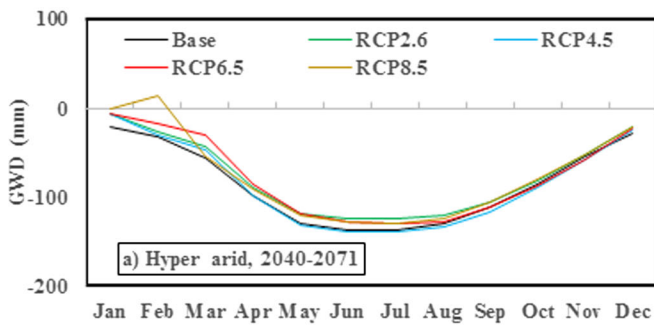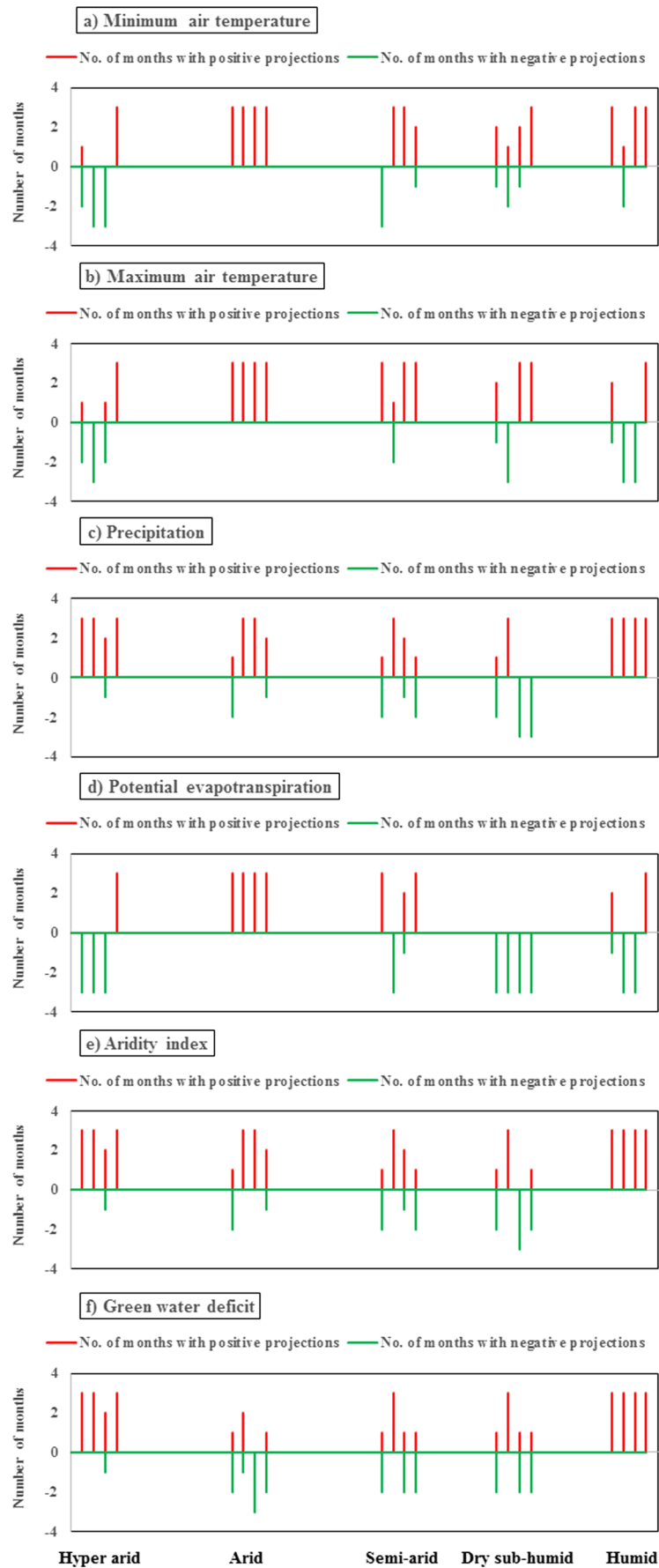rming may be provided within the hyper-arid and humid regions, since global warming projects a significant reduction in the severity condition, and a positive increase in green water availability in these regions over the 2041–2070 period.

Nevertheless, it should be noted that P and T variations need to be considered individually as well, when the land suitability for dry farming is determined in the future period. In fact, not improved condition may be expected if proper solutions under the positive or negative changes in P or T are not adopted. For example, the summarized results in Table 2 well represents that Iran may experience a 17.5–36.5% increase in annual P over the 2041–2070 period, which may be considered as a positive sign of increased potentials for rainfed farming under global warming. However, such increase is supposed to mainly happen over the wet seasons, which may result in serious natural hazards such as waterlogging (Fig. 5). On the other hand, monthly P analysis within the hyper-arid and humid regions also reveals a significant increase in monthly P over the dry seasons (Figs. 3 and 5), which may consequently lead to weeds and pest growths and soil erosion due to reduced soil water availability (Karandish et al. 2017a; Enete and Amusa 2010). Hence, expanding dry farming within the proper climatic regions requires implementing long-term planning for controlling the probable negative consequences of projected P in those regions.

Air temperature (T) is also a highlighted factor, which affects soil-water-crop relationships. Based on the ensemble average of the 20 GCMs and four RCPs, the arid and semi-arid regions, which have the largest contribution in total rainfed and irrigated production, may experience a considerable increase in both Tmin and Tmax, especially over the wet seasons. While increased T is reported to result in crop water requirement reduction caused by the reduced length of the

a) Minimum air temperature

── No. of months with positive projections   ── No. of months with negative projections

Number of months

b) Maximum air temperature

── No. of months with positive projections   ── No. of months with negative projections

Number of months

c) Precipitation

── No. of months with positive projections   ── No. of months with negative projections

Number of months

d) Potential evapotranspiration

── No. of months with positive projections   ── No. of months with negative projections

Number of months

e) Aridity index

── No. of months with positive projections   ── No. of months with negative projections

Number of months

f) Green water deficit

── No. of months with positive projections   ── No. of months with negative projections

Number of months

Hyper arid   Arid   Semi-arid   Dry sub-humid   Humid

cropping cycles (Karandish et al. 2017a, b; Darzi-Naftchali and Karandish 2017), the elevated T may result in irreparable losses as well due to its negative effect on crop growth and yield. Cardinal temperatures (i.e., Tmin and Tmax) may affect cropping calendar since there is a crop-specific T thresholds, within which crops may achieve their highest growth and yield. Hence, any change in these thresholds may avoid crops to complete a specific phonological phase or their whole life cycle (Luo 2011). On the other hand, the growth of weeds, pests, and insects is highly depended on air temperature, especially within the wet seasons, all of which may led to a significant loss in crop yield (Pradhan et al. 2012; Luo 2011; Selvaraj et al. 2011; Wahid et al. 2007; Ugarte et al. 2007; Vollenweider and Gunthardt-Goerg 2005; Peng et al. 2004; Shah and Paulsen 2003; Commuri and Jones 2001; Wheeler et al. 2000; Stone and Nicolas 1995; Baker and Allen 1993). Reduced cardinal temperature, which is evident for 2–8 months in different climatic regions, may also be an obstacle to proper crop growth, or to the move of water and nutrients in soil (Karandish and Shahnazari 2016; Callejas et al. 2009; Lathi et al. 2005; Puhe 2003; Dong et al. 2001; Pregitzer et al. 2000; Psarras et al. 2000), all of which result in lowered yield compared to the favorable condition (Aphalo et al. 2006; Schwarz et al. 1997).

While climate variables are proper and unavoidable indices for assessing dry farming suitability within a specific region in the future, they may not to be enough since global warming may change crop CO_2 intake, which is reported to have a significant effect on crop yield (Anwar et al. 2013; Trnka et al. 2004). Being a proper index of farmers' economic prosperity, crop yield then need to be anticipated under climate change as well. In other words, even if a region is assessed to be suitable for dry farming, the policy makers, or even the local farmers, may avoid adopting such decision if their financial interests are not fulfilled. Regarding these points, applying crop growth models for simulating crop yield in the future period let one to consider the probable consequences of projected P and T on crop growth and yield as well. Hence, it is supposed to include economic indices together with climate variables when new targets for expanding dry farming is considered.

4 Conclusion

Climate change researches are mainly focused on determining future projections main weather data, including precipitation, temperature, and/or reference evapotranspiration. While being a key factor for determining the suitability of dry farming within a region, less attention has been paid to determine the

future projections of aridity index and/or green water deficit. In addition, most of the previous researches provided climate change projections based on the results of a few GCMs and emission scenarios. However, there will be a large spatial and temporal heterogeneities in climate change projections under different GCMs and scenarios, due to different properties of these model and/or different assumptions embodied in these models and scenarios. Hence, achieving more reliable results requires predicting climate change projections based on a wide range of GCMs and emission scenarios. This research is noble in a way that, (i) first, we included AI and GWD indices, in addition to main weather data, in our assessment when determining dry-farming suitability under global warming; (ii) and second, we considered the outputs of 80 ensembles (20 GCMs and 4 emission scenarios) in our analysis, which let us providing more reliable results for the uncertain future.

To address the considered objectives in this research, the annul and monthly P, Tmin, Tmax, ETo, AI, and GWD projections were analyzed for five climatic zone of Iran, based on the outputs of 20 GCMs under four RCPs scenarios of RCP2.6, RCP4.5, RCP6.5, and RCP8.5. Together with agricultural data, these projections were then applied to regionally determine the dry farming suitability over the mid twenty-first century (i.e., 2041–2070). The most important concluding remarks may be summarized as in the following:

- Regardless of the climatic regions, annual climate change projections mainly show a positive increase in both precipitation and air temperature, while both negative and positive projections in these variables are observed at the monthly time-scale.
- The arid and semi-arid regions are the most vulnerable regions to climate change, since they are mainly subjected to a significant reduction in green water availability, and a substantial increase in drought condition, especially over the wet seasons.
- The policy makers may need to consider expanding dryland agriculture within the hyper arid region, which is the most water scarce region of the country over the base period, since it may experience a considerable improved climatic condition for producing rainfed crops over the mid twenty-first century.
- While the humid region may be the most suitable region for rainfed cultivation, their improper cropping pattern caused this area to be the largest irrigated-rice producer under current condition, which exposed a severe pressure into the blue water resources. Hence, prioritizing the current cropping pattern may be of priority under global warming, especially within the water-abundant regions of the country.
- Climate change researches are required to be carried out based on a wide range of GCMs and RCPs in order to

reduce the risk of long-term project failures, since our results show a wide range of positive and negative projections into the basic climatic variables, as well as into the drought indices, under different GCMs and RCPs.

- The severity of climate change projections highly varies by space and time, and not a constant pattern is followed up. Such results well indicated the highlighted importance of regional studies over the future periods, when successful projects are managed.

- Together with climatic suitability for dryland agriculture, the economic indices may need to be included in further approaches as well, when implementing new targets for expanding rainfed cropping within the right areas.

References

Ahani H, Kherad M, Kousari MR, Roosmalen LV, Aryanfar R, Hosseini SM (2013) Non-parametric trend analysis of the aridity index for three large arid and semi-arid basins in Iran. Theor Appl Climatol 112:553–564

Allen RG, Pereira LS, Raes D, Smith M (1998) Crop evapotranspiration: guidelines for computing crop water requirements. In: FAO irrigation and drainage paper no. 56. FAO, Rome, pp 300

Anwar MR, Liu DL, Macadam I, Kelly G (2013) Adapting agriculture to climate change: a review. Theor Appl Climatol 113(1–2):225–245

Aphalo PJ, Lahti M, Lehto T, Repo T, Rummukainen A, Mannerkoski H, Finer L (2006) Responses of silver birch saplings to low soil temperature. Silva Fenn 40(3):429–442

Ashraf B, Yazdani R, Mousavi-Baygi M, Bannayan M (2014) Investigation of temporal and spatial climate variability. Theor Appl Climatol 118:35–46

Baker JT, Allen LH Jr (1993) Effects of CO_2 and temperature on rice. J Agric Meteorol 48(5):575–582

Callejas R, Pablo Canales P, de Cortazar VG, dC G (2009) Relationship between root growth of Thompson seedless grapevines and soil temperature. Chil J Agr Res 69(4):496–502

Chiyuan M, Qingyun D, Qiaohong S, Yong H, Dongxian K, Tiantian Y, Aizhong Y, Zhenhua D, Wei G, (2014) Assessment of CMIP5 climate models and projected temperature changes over Northern Eurasia. Environmental Research Letters 9 (5):055007

Commuri PD, Jones RD (2001) High temperatures during endosperm cell division in maize: a genotypic comparison under in vitro and field conditions. Crop Sci 41:1122–1130

Darzi-Naftchali A, Karandish F (2017) Adapting rice production to climate change for sustainable blue water consumption: an economic and virtual water analysis. Theor Appl Climatol. https://doi.org/10.1007/s00704-017-2355-7

Dong S, Scagel CF, Cheng L, Fuchigami L, Rygiewicz PT (2001) Soil temperature and plant growth influences nitrogen uptake and aminoacid concentration of apple during early spring growth. Tree Physiol 21(8):541–547

Dong J, Liu J, Zhang G, Basara JB, Greene S, Xiao X (2013) Climate change affecting temperature and aridity zones: a case study in Eastern Inner Mongolia, China from 1960–2008. Theor Appl Climatol 113:561–572

Enete AA, Amusa TA, (2010) Challenges of agricultural adaptation to climate change in Nigeria: a synthesis from the literature», field actions science reports [online], URL: http://factsreports.revues.org/678

Gebremedhin MA, Abraha AZ, Fenta AA (2017) Changes in future climate indices using statistical downscaling model in the upper Baro basin of Ethiopia. Theor Appl Climatol 133:39–46. https://doi.org/10.1007/s00704-017-2151-4

IMAJ (2017) Iran's Ministry of Agriculture Jihad, Tehran, Iran. www.maj.ir

IPCC (2013) Climate change 2013: the physical science basis. In: Stocker TF, Qin D, Plattner G-K, Tignor M, Allen SK, Boschung J, Nauels A, Xia Y, Bex V, Midgley PM (eds) Contribution of working group I to the fifth assessment report of the intergovernmental panel on climate change. Cambridge University Press, Cambridge and New York, pp 1535. https://doi.org/10.1017/CBO9781107415324

IRIMO (2017) Iran meteorological organization, Tehran, Iran, www.irimo.ir/f

Jones PD, Osborn TJ, Briffa KR (1997) Estimating sampling errors in large-scale temperature averages. J Clim 10(10):2548–2568

Karandish F, Hoekstra AY (2017) Informing national food and water security policy through water footprint assessment: the case of Iran. Water 9(11):831

Karandish F, Mousavi SS (2018) Climate change uncertainty and risk assessment in Iran during twenty-first century: evapotranspiration and green water deficit analysis. Theor Appl Climatol 131(1-2):777–791

Karandish F, Shahnazari A (2016) Soil temperature and maize nitrogen uptake improvement under partial root zone drying. Pedosphere 26(6):872–886

Karandish F, Mousavi SS, Tabari H (2017a) Climate change impact on precipitation and cardinal temperatures in different climatic zones in Iran: analyzing the probable effects on cereal water-use efficiency. Stoch Environ Res Risk Assess 31:2121–2146. https://doi.org/10.1007/s00477-016-1355-y

Karandish F, Kalanaki M, Saberali SF (2017b) Projected impacts of global warming on cropping calendar and water requirement of maize in a humid climate. Arch Agron Soil Sci 63(1):1–13

Keyantash J, Dracup JA (2002) The quantification of drought: an evaluation of drought indices. Bull Am Meteorol Soc 83:1167–1180

Lathi M, Aphalo PJ, Finer L, Ryyppo A, Lehto T, Mannerkoski H (2005) Effects of soil temperature on shoot and root growth and nutrient uptake of 5-year-old Norway spruce seedlings. Tree Physiol 25:115–122

Li R, Tsunekawa A, Tsubo M (2017) Assessment of agricultural drought in rainfed cereal production areas of northern China. Theor Appl Climatol 127(3–4):597–609

Liu X, Zhang D, Luo Y, Liu C (2013) Spatial and temporal changes in aridity index in northwest China: 1960 to 2010. Theor Appl Climatol 112:307–316

Liu Q, Yan C, Ju H, Garre S (2017) Impact of climate change on potential evapotranspiration under a historical and future climate scenario in the Huang-Huai-Hai Plain, China. Theor Appl Climatol 132:387–401. https://doi.org/10.1007/s00704-017-2060-6

Luo Q (2011) Temperature threshold and crop production: a review. Clim Chang 109:583–598

Milly PCD, Dunne KA, Vecchia AV (2005) Global pattern of trends in streamflow and water available in a changing climate. Nature 438:347–350

Moral FJ, Rebollo FJ, Paniagua LL, García-Martín A, Honorio F (2016) Spatial distribution and comparison of aridity indices in Extremadura, southwestern Spain. Theor Appl Climatol 126(3–4):801–814

Muhire I, Ahmed F (2016) Spatiotemporal trends in mean temperatures and aridity index over Rwanda. Theor Appl Climatol 123(1–2):399–414

Paltineanu C, Mihailescu IF, Seceleanu I (2007) Using aridity indices to describe some climate and soil features in Eastern Europe: a

Romanian case study. Theor Appl Climatol 90:263–274. https://doi.org/10.1007/s00704-007-0295-3

Peng S, Huang J, Sheehy JE, Lanza RC, Visperas RM, Zhong X, Centeno GS, Khush GS, Cassman KG, (2004) Rice yields decline with higher night temperatures from global warming. Proc Natl Acad Sci USA. http://www.pnas.org/cgi/content/full/101/27/9971. 10 pp.

Pradhan GP, Prasad PVV, Fritz AK, Kirkham MB, Gill BS (2012) High temperature tolerance in Aegilops species and its potential transfer to wheat. Crop Sci 52:292–304

Pregitzer KS, King JS, Burton AJ, Brown SE (2000) Responses of tree fine roots to temperature. New Phytol 147:105–115

Psarras G, Merwin IA, Lakso AN, Ray JA (2000) Root growth phenology, root longevity and rhizosphere respiration of field grown "Mutsu" apple trees on "mailing 9" rootstock. J Am Soc Hortic Sci 125:596–602

Puhe J (2003) Growth and development of the root system of Norway spruce (Picea abies) in forest stands—a review. For Ecol Manag 175:253–273

Salark N, Mahmood-Agha OMA (2017) Spatial and temporal variations of aridity indices in Iraq. Theor Appl Climatol 133:89–99. https://doi.org/10.1007/s00704-017-2163-0

Schwarz PA, Fahey TJ, Dawson TE (1997) Seasonal air and soil temperature effects on photosynthesis in red spruce (Picea rubens) saplings. Tree Physiol 17:187–194

Selvaraj IC, Nagarajan P, Thiyagarajan K, Bharathi M, Rabindran R (2011) Genetic parameters of variability, correlation and path coefficient studies for grain yield and other yield attributes among rice blast disease resistant genotypes of rice (Oryza Sativa L.). Afr J Biotechnol 10:3322–3334

Shah NH, Paulsen GM (2003) Interaction of drought and high temperature on photosynthesis and grain-filling of wheat. Plant Soil 257: 219–226

Shifteh Some'e B, Ezani A, Tabari H (2013) Spatiotemporal trends of aridity index in arid and semi-arid regions of Iran. Theor Appl Climatol 111(1-2):149–160

Stone PJ, Nicolas ME (1995) Effect of timing of heat stress during grain filling on two wheat varieties differing in heat tolerance. I. Grain growth. Aust J Plant Physiol 22:927–934

Tabari H, Aghajanloo M-B (2013) Temporal pattern of aridity index in Iran with considering precipitation and evapotranspiration trends. Int J Climatol 33:396–409

Tabari H, Hosseinzadeh Talaee P (2013) Moisture index for Iran: spatial and temporal analyses. Glob Planet Chang 100:11–19

Tabari H, Taye MT, Willems P (2015) Water availability change in central Belgium for the late 21st century. Glob Planet Chang 131:115–123

Tigkas D, Vangelis H, Tsakiris G (2018) Drought characterisation based on an agriculture-oriented standardised precipitation index.

Theoretical and Applied Climatology. https://doi.org/10.1007/s00704-018-2451-3

Trnka M, Dubrovsky M, Semeradove D, Zalud Z (2004) Projections of uncertainties in climate change scenarios into expected winter wheat yields. Theor Appl Climatol 77(3–4):229–249

Trzaska S, Schnarr E (2014) A review of downscaling methods for climate change projections: African and Latin American resilience to climate change (ARCC). http://www.ciesin.org/documents/Downscaling_CLEARED_000.pdf. Accessed date: March 2015

Ugarte C, Calderini DF, Slafer GA (2007) Grain weight and grain number responsiveness to preanthesis temperature in wheat, barley and triticale. Field Crop Res 100:240–248

UNESCO: United Nations Educational, Scientific and Cultural Organization (1979) Map of the world distribution of arid regions: explanatory note. MAB technical notes. UNESCO, Paris

Vollenweider P, Gunthardt-Goerg MS (2005) Diagnosis of abiotic and biotic stress factors using the visible symptoms in foliage. Env Pollut 137:455–465

Wahid A, Gelani S, Ashraf M, Foolad MR (2007) Heat tolerance in 1260 plants: an overview. Environ Exp Bot 61:199–223

Wang LZ, Cao LG, Deng XJ, Jia PH, Zhang W, Xu XWH, Zhang KX, Zhao YF, Yan BJ, HuW CYY (2014) Changes in aridity index and reference evapotranspiration over the central and eastern Tibetan Plateau in China during 1960–2012[J]. Quatern Sci 349:280–286

Wegren SK (2011) Food security and Russia's 2010 drought. Eurasian Geogr Econ 52(1):140–156

Wheeler TR, Craufurd PQ, Ellis RH, Porter JR, Vara Prasad PV (2000) Temperature variability and the yield of annual crops. Agric Ecosyst Environ 82:159–167

WMO and GWP: World Meteorological Organization and Global Water Partnership (2016) Handbook of drought indicators and indices. In: Svoboda M, Fuchs BA (eds) Integrated drought management Programme (IDMP). Integrated drought management tools and guidelines series 2, Geneva

Zhang K, Qian Z, Liu P, Xu Y, Cao L, HAo Y, Dai S (2017a) Variation characteristics and influences of climate factors on aridity index and its association with AO and ENSO in northern China from 1961 to 2012. Theor Appl Climatol 130(1–2):523–533

Zhang Q, Zhang J, Wang C (2017b) Risk assessment of drought disaster in typical area of corn cultivation in China. Theor Appl Climatol 128(3–4):533–540

Zhao M, Running SW (2010) Drought-induced reduction in global terrestrial net primary production from 2000 through 2009. Science 329(5994):940–943

Zhao Y, Zou X, Cao L, Yao Y, Fu G (2017) Spatiotemporal variations of potential evapotranspiration and aridity index in relation to influencing factors over Southwest China during 1960–2013. Theor Appl Climatol. https://doi.org/10.1007/s00704-017-2216-4